A Three Dimensional (Time, Wavelength and Intensity) Functioning Fluorescent Probe for the Selective Recognition/Discrimination of Cu^{2+}, Hg^{2+}, Fe^{3+} and F^- ions†

Qin Ruan,[a] Lan Mu,[a] Xi Zeng,*[a] Jiang-Lin Zhao,*[b] Zhen-Min Chen,[b] Gang Wei*[c] and Carl Redshaw[d]

[a] Key Laboratory of Macrocyclic and Supramolecular Chemistry of Guizhou Province; School of Chemistry and Chemical engineering, Guizhou University, Guiyang 550025, China. E-mail: zengxi1962@163.com
[b] Shenzhen Institutes of Advanced Technology, Chinese Academy of Sciences, 1068 Xueyuan Avenue, Shenzhen 518055, China. E-mail: zhaojianglin1314@163.com
[c] CSIRO Manufacturing, PO Box 218, NSW 2070, Australia. E-mail: gang.wei@csiro.au
[d] Department of Chemistry, School of Mathematics and Physical Sciences, University of Hull, Hull HU6 7RX, U.K.

WE HAVE STRATEGICALLY INCORPORATED THREE DIFFERENT FLUOROPHORES AT TREN TO CONSTRUCT A MULTI-ENERGY DONOR/ACCEPTOR "SMART" PROBE L. THIS PROBE OPERATES BY USING THREE DIMENSIONAL SCALES (response time, wavelength and fluorescence intensity) which allows for the SELECTIVE RECOGNITION AND DISCRIMINATION OF THE IONS Cu^{2+}, Hg^{2+}, Fe^{3+} and F^-.

Fluorescent probes are widely used as powerful tools for molecular recognition due to their high selectivity, sensitivity, simplicity in manipulation and their capacity for real-time imaging and non-destructive nature.[1] Over the past few decades, various fluorescent probes have been developed, based on different mechanisms such as photoinduced electron transfer (PET),[2] excimer/exciplex formation or extinction (Excimer),[3] intramolecular charge transfer (ICT),[4] aggregation induced emission (AIE) [5] and fluorescence (Förster) resonance energy transfer (FRET). [6] Based on their differing analytical capabilities, such probes can recognize a mono-target guest,[7] di-target guests,[8] tri-target guests[9] and even more. They can be prepared by either organic synthesis[10] or inorganic synthesis (quantum dot).[11] However, despite the diversity of probes reported, they all function basically by using either fluorescence wavelength or intensity changes (two dimensional scales). Herein, we would like to introduce the use of three dimensional scales (time, wavelength and intensity) for the selective recognition and discrimination of guest ions using the FRET fluorescent probe **L**. To the best of our knowledge, this type of fluorescent probe has not been reported previously.

The multi-energy donor and acceptor "smart" probe **L**, incorporates three different fluorophores, *i.e.* 7-hydroxy-2-oxo-*2H*-chromene-8-carbaldehyde (Coumarin), 7-nitrobenz-2-oxa-1,3-diazole (NBD) and rhodamine-B (Rh-B), which act as the excitation energy donor and acceptor components (Fig. 1). The fluorophores were selected based on the spectral overlap between the radiative emission of the donor and the absorbance of the acceptor (Fig. S4); this can efficiently induce fluorescence resonance energy transfer (FRET). The three different fluorophores were introduced in three steps; synthetic details are given in the supporting information (Scheme S1). **L** has been fully characterized by ^1H and ^{13}C NMR spectroscopy and by mass spectrometry (Figs. S1 ~ S3).

For fluorescent probes, both high selectivity and sensitivity are important attributes. Herein, there are two possible donor groups, *i.e.* coumarin and NBD, in other words, there are two different excitation wavelengths $\lambda_{ex\ (Coumarin)}$ = 365 nm and $\lambda_{ex\ (NBD)}$ = 470 nm. Hence, we initially investigated the selectivity and sensitivity of probe **L** by the fluorescent method at the excitation wavelength of coumarin ($\lambda_{ex\ (Coumarin)}$ = 365 nm, Fig. 2a). Probe **L** (20 μM) exhibited almost no fluorescence in CH_3CN/H_2O (97/3, v/v, pH = 7) due to the PET process. Upon the addition of various metal cations (Li^+, Na^+, K^+, Ag^+, Mg^{2+}, Ca^{2+}, Sr^{2+}, Ba^{2+}, Zn^{2+}, Co^{2+}, Ni^{2+}, Pb^{2+}, Hg^{2+}, Cu^{2+}, Cr^{3+}, Al^{3+} and Fe^{3+}), there were no detectable changes, except on addition of Hg^{2+}, Fe^{3+} and Cu^{2+}. In particular, the addition of Hg^{2+} resulted in an immediate (within 2 mins a 100-fold increase) acute fluorescent enhancement at 585 nm (the characteristic emission of Rh-B due to the spirolactam ring-opening), which was accompanied by a stable orange coloured "turn on" fluorescence under a UV-vis lamp (365nm). This indicated that
the Rh-B spirolactam ring was opened and resulted in an effective FRET process. Interestingly, in the presence of Fe^{3+} and Cu^{2+}, there is a slower start to the process (Fig. 2b). Over time, the presence of Fe^{3+} starts to induce a slow fluorescent enhancement at 525nm and 585 nm. After about 75 min, a stable fluorescence emission is achieved, and its intensity at 585 nm is higher than that observed in the presence of Hg^{2+}. In contrast, the presence of Cu^{2+} did not bring about a significant fluorescent change at 585 nm even over longer time periods, but did trigger a gradually fluorescence increase at 525 nm (the characteristic emission of NBD). It also reached a plateau after about 100 minutes, and a stable green colour fluorescence can be observed. All of these observation indicated that probe **L** can

initiate three different FRET recognition modes dependent on the different target ions present, *viz* recognition of Hg^{2+} via the Rh-B moiety (585 nm), Fe^{3+} via both the Rh-B (585 nm) and NBD moieties (525 nm), whilst Cu^{2+} is only through the NBD moiety (525 nm). Similar phenomenon can be observed when we tuned the excitation wavelength to 470 nm ($\lambda_{ex(NBD)}$), except that the fluorescence intensity was stronger (Fig. S5). This stronger fluorescence maybe attributed to the fact that the overlap of the spectral area of NBD/Rh-B is larger than that of coumarin/Rh-B (Fig. S4), which resulted in a higher efficient FRET process.

In order to investigate these three different FRET "OFF-ON" systems, fluorescent titration experiments have been carried out. Upon increasing the concentration of Hg^{2+} in a solution of probe **L** (Fig. 3a), the emission maximum shifted from 525 nm (characteristic of NBD, weak emission due to the PET effect) to 585 nm (characteristic of Rh-B, the acute enhancement is attributed to the Hg^{2+}-induced FRET) *via* an intermediate chelation process with a characteristic emission band at about 555 nm (upon addition of 0.1 equiv. of Hg^{2+}). It reached equilibrium after the addition of 1.0 equiv. Hg^{2+} which suggested a 1:1 complex stoichiometry for the Hg^{2+}·Rh-B—**L** complex (Fig. 3a inset). Interestingly, when Fe^{3+} was added to the solution of probe **L**, at the beginning (0 to 1.0 equiv.), there was no significant fluorescence change at 585 nm, but it did exhibit a detectable fluorescent enhancement at 525 nm which maybe ascribed to the inhibition PET process of the NBD fluorophore (Fig. 3b). On increasing the concentration of Fe^{3+} from 1.0 to 2.0 equiv., a dramatically fluorescence enhancement was observed at 585 nm, which indicated the Fe^{3+}-induced spirolactam ring-opening of Rh-B moiety during this process. Further increasing Fe^{3+} (>2.0 equiv.) did not bring

any significant changes in the fluorescent spectrum, which suggested that the complex system had reached equilibrium. Hence, these observation indicated that there is a two-step complex process for probe **L** and Fe^{3+}: firstly, probe **L** complexes with one equiv. of Fe^{3+} through the NBD moiety forming an Fe^{3+}·NBD—**L** intermediate complex, and then further complexes Fe^{3+} through the Rh-B moiety to form the final stable 1:2 Fe^{3+}·NBD—**L**—Rh-B·Fe^{3+} complex. It is perhaps this two-step complex process which results in the longer observed response time for the detection of Fe^{3+} by probe **L**. The significant emission at 585 nm (Rh-B) and a relatively weaker emission band at 525 nm (NBD) appeared, which suggested that two FRET processes were occurring between coumaring-Rh-B and coumaring-NBD. However, on increasing the amount of Cu^{2+} cation in the solution of probe **L**, a green fluorescence was induced which was ascribed to the emission of the NBD fluorophore at 525 nm (Fig. 3c, to more fully explore the complexation process, the 470 nm excitation titration results are shown.). The results strongly suggest that the probe **L**·Cu^{2+} complex was formed through the NBD moiety, *i.e.* Cu^{2+}·NBD—**L**. The 1:1 complex stoichiometry for Cu^{2+}·**L** complex was supported by a Job's plot (Fig. S6).

On the other hand, in order to fully investigate the recognition capability of probe **L**, studies of probe **L** towards anions have been carried out in CH_3CN solution (Fig. 4). Regardless of whether 365 nm or 470 nm were employed as the excitation wavelength, there was only a very weaker fluorescence at about 525 nm ($I_{\lambda 365\ nm} = 30$ and $I_{\lambda 470\ nm} = 95$) for probe **L**. Interestingly, upon the addition of F^- anions, the different excitation wavelength resulted in different phenomenon. When 365 nm was employed as the excitation wavelength, the fluorescence exhibited an acute increase at 460 nm, which indicated that the coumarine participates in the complexation of F^- (Fig. 4a). In contrast, when 470 nm was selected as the excitation wavelength, the fluorescence at 525 nm decreased upon the addition of F^- which suggested that the NBD moiety also participated in the complexation process (Fig. S7). The fluorescent titration experiments revealed the detail complex process (Fig. S8), namely that the F^- anion was complexed by the *OH* group at the coumarine moiety and the *NH* group at the NBD moiety via hydrogen bonding. This binding interaction locks the C=N bond of probe **L** in place, preventing its rapid isomerisation and switching the fluorescence 'on'.

To further investigate the practical applicability of probe **L** (20 μM) as a Hg^{2+}, Fe^{3+}, Cu^{2+} and F^- ion selective fluorescent probe, competitive experiments were carried out. As shown in Fig. S9, no significant interference to the selective response of probe **L** to Hg^{2+}, Fe^{3+}, Cu^{2+} or F^- ion were observed in the presence of any of the other ions employed herein when using the three dimensional scales (time, wavelength and intensity) method. Upon the addition of probe **L** to the detection solution, if we observed an acute enhancement and stable fluorescence at 585 nm (orange coloured solution) over two minutes, this is suggestive of the presence of Hg^{2+}. By contrast, if we observe a gradual enhancement (over about 100 min) at 585 nm and 525 nm, this is consistent with the presence of Fe^{3+}; on the other hand, if we only observe a fluorescence enhancement at 525 nm (a green coloured solution), this suggests the presence of Cu^{2+}. Furthermore, if we observe a fluorescent enhancement at 460 nm (a cyan coloured solution), this indicates the presence of F^- anion. In other words, probe **L** can act as a highly efficient three dimensional scale fluorescent probe for the recognition and discrimination of Cu^{2+}, Hg^{2+}, Fe^{3+} and F^- ions.

Under the optimal conditions, the detection of linear relationships and limits of detection (LOD = 3σ /slope) for probe **L** with Hg^{2+}, Fe^{3+}, Cu^{2+} and F^- are summarized in Table S1. This data suggests that probe **L** is also a sensitive fluorescent probe for the recognition and discrimination of these four ions. A binding analysis using the method of continuous variations established a 1:1 for **L**·Hg^{2+}, 1:2 for **L**·2Fe^{3+} and 1:1 for **L**·Cu^{2+} complex formation. The complexations were further confirmed by MALDI-TOF mass spectrometry. Mass peaks at *m/z* 1105.28056 (calculated value 1105.34104), *m/z* 1017.25709 (calculated value 1017.25594) and *m/z* 969.30535 (calculated value 969.32349) were observed, which corresponded to [**L** + Hg -2 H]$^+$, [**L** + 2Fe]$^{6+}$ and [**L** + Cu + H]$^{3+}$ complexes (Fig. S10), respectively. Combining all of these observation, we proposed the possible binding mode for **L**·Hg^{2+}, **L**·2Fe^{3+}, **L**·Cu^{2+} and **L**·F^- as shown in Figure 5.

The capability of probe **L** to detect Hg^{2+}, Fe^{3+} and Cu^{2+} within living cells was investigated by fluorescence imaging on a fluorescent inverted microscope. Bright-field measurements confirmed that the cells, after being treated with Hg^{2+}, Fe^{3+}, Cu^{2+} and **L**, were viable throughout the imaging experiments. In the control experiment, human prostatic cancer cells (PC3) with a 10 μM probe **L** over 50 min led to negligible intracellular fluorescence (Fig. 6a and 6b). When the cells were first incubated with 10 μM probe **L** for 50 min, and then further treated with 50 μM of metal ions (Hg^{2+}, Fe^{3+} or Cu^{2+}) for another 40 ~ 50 min, a significant increase in the fluorescence from the intracellular area was observed (Fig. 6c, ~ 6f). These results demonstrate that the probe is permeable to cells, binds to intracellular Hg^{2+}, Fe^{3+} and Cu^{2+}, and emits strong fluorescent light, and thus it is highly suitable for determining intracellular Hg^{2+}, Fe^{3+} and Cu^{2+} ions. The responses to Hg^{2+}, Fe^{3+} and Cu^{2+} ions exhibited distinctly different colours (red and green, respectively) for the cell samples and this raises the prospect that the Hg^{2+}, Fe^{3+} or Cu^{2+} ions could be simultaneously determined.

In conclusion, a multi-analyse probe **L** for the recognition and discrimination of the four ions Hg^{2+}, Fe^{3+}, Cu^{2+} and F^{-}, without any interference from other potentially competing ions according to their response time, max wavelength and fluorescent intensity, has been successfully obtained. Cell imaging demonstrated that probe **L** can be further used for monitoring intracellular Hg^{2+}, Fe^{3+} and Cu^{2+} levels in living cells. To the best of our knowledge, this is the first case of utilizing the three dimensional scales (time, wavelength and intensity) to recognize and discriminate different ions with a single fluorescent probe; previous reports normally involve the two dimensional scales (wavelength and intensity). Our study illustrates an effective and novel strategy to differentiate multi-analyses. This work provides a promising new strategy for the simultaneous detection of ions by one simple probe.

This work was supported by the "Chun-Hui" Fund of Chinese Ministry of Education (Z2015007 & Z2016008), SIAT Innovation Program for Excellent Young Researchers (2017014) and the Innovation Fund of the Graduate Student of Guizhou University (2017002).

Notes and references

1 (*a*) Z. Yang, J. Cao, Y. He, J. H. Yang, T. Kim, X. Peng and J. S. Kim, *Chem. Soc. Rev.*, 2014, **43**, 4563; (*b*) J. Li, D. Yim, W. D. Jang and J. Yoon, *Chem Soc Rev*., 2017, **46**, 2437; (*c*) X. Chen, F. Wang, J. Y. Hyun, T. Wei, J. Qiang, X. Ren, I. Shin and J. Yoon, *Chem. Soc. Rev.*, 2016, **45**, 2976.

2 (*a*) J. Zhu, S. Sun, K. Jiang, Y. Wang, W. Liu and H. Lin, *Biosens. Bioelectron*., 2017, **97**, 150; (*b*) S. Adhikari, A.Ghosh, M. Ghosh, S. Guria and D. Das, *Sensor. Actuat. B-chem*., 2017, **251**, 942; (*c*) C. Liua, X. Jiao, S. He, L. Zhao and X. Zeng, *Talanta*., 2017, **174**, 234.

3 (*a*) J.-L. Zhao, H. Tomiyasu, C. Wu, H. Cong, X. Zeng, S. Rahman, P. E. Georghiou, D. L. Hughes, C. Redshaw and T. Yamato, *Tetrahedron*., 2015, **71**, 8521; (*b*) W. Lu, C. Ma, Z. Li, J. Zhang, Y. Huang, Q. Huang and T. Chen, *Sensor. Actuat. B-chem*., 2017, **246**, 631.

4 (*a*) Y.-T. Wu, J.-L. Zhao, L. Mu, X. Zeng, G. Wei, C. Redshaw, and Z. Jin, *Sensor. Actuat. B-chem.*, 2017, **252**, 1089; (*b*) N. I. Georgiev, M. D. Dimitrova, P. V. Krasteva and V. B. Bojinov, *J Lumin.*, 2017, **187**, 383.

5 (*a*) J. Shi, Q. Deng, C. Wan, M. Zheng, F. Huang and B. Tang, *Chem. Sci.*, 2017, **8**, 6188; (*b*) Y.-Q. Niu, T. He, J. Song, S.-P. Chen, X.-Y. Liu, Z.-G. Chen, Y.-J. Yu and S.-G. Chen, *Chem. Commun.*, 2017, **53**, 7541.

6 (*a*) B. Dong, X. Song, C. Wang, X.i Kong, Y. Tang, and W. Lin, *Anal. Chem*. 2016, **88**, 4085; (*b*) Y. Ge, A. Liu, R. Ji, S. Shen and X. Cao, *Sensor. Actuat. B-chem.*, 2017, **251**, 410.

7 (*a*) J. Wang, R. S. Li, H. Z. Zhang, N. Wang, Z. Zhang and C. Z. Huang, *Biosens. Bioelectron.*, 2017, **97**, 157; (*b*) Z. Gao, B. Han, K. Chen, J. Sun and X. Hou, *Chem. Commun.*, 2017, **53**, 6231.

8 (*a*) K. Mahesh and S. Karpagam, *Sensor. Actuat. B-chem.*, 2017, **251**, 9; (*b*) Y. Tang, J. Sun and B. Yin, *Anal Chim Acta*., 2016, **942**, 104.

9 (*a*) N. R. Chereddy, P. Nagaraju, M.V. Niladri Raju, V. R. Krishnaswamy, P. S. Korrapati, P. R. Bangal, and V. J. Rao, *Biosens. Bioelectron.*, 2015, **68**, 749; (*b*) J. Wang, Y. Li, N. G. Patel, G. Zhang, D. Zhou and Y. Pang, *Chem Commun.*, 2014, **50**, 12258.

10 (*a*) K. Huang, Y. Yue, X. Jiao, C. Liu, Q. Wang, S. He, L. Zhao and X. Zeng, *Dyes Pigments*., 2017, **143**, 379; (*b*) X. He, Y.Hu, W. Shi, X. Li and H. M, *Chem. Commun.*, 2017, **53**, 9438.

11 (*a*) J. Zhu, S. Sun, K. Jiang, Y. Wang, W. Liu, and H. Lin, *Biosens. Bioelectron*., 2017, **97**, 150; (*b*) L. Chang, X. He, L. Chen and Y. Zhang, *Sensor. Actuat. B-chem*., 2017, **250**, 17.

Figures and Captions

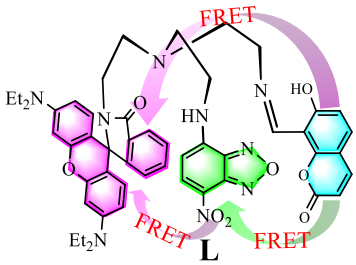

Figure 1. The molecular structure of probe **L**.

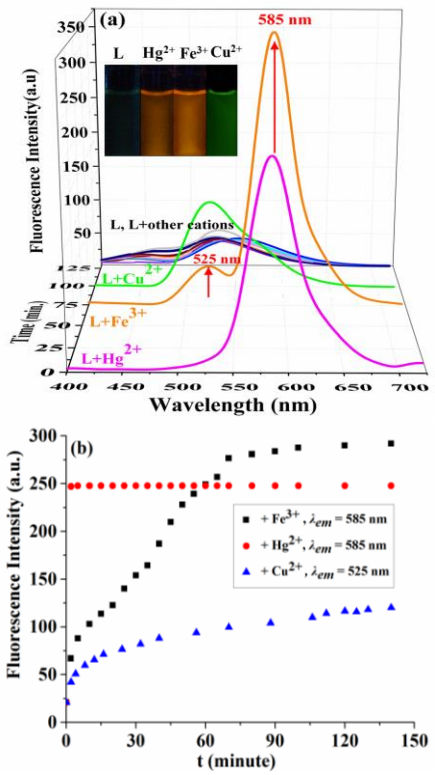

Figure 2. (a) Fluorescence spectrum of probe **L** (20 μM) with 20 equiv. of different metal ions (measured after equilibrium, λ_{ex} = 365 nm) in CH_3CN/H_2O (97/3, v/v, Tris-HCl, pH 7) solution; (b) The fluorescence intensity of probe **L** on addition of 20 equiv. of Hg^{2+} (λ_{ex}/ λ_{em} = 365 nm/ 585 nm), Fe^{3+} (λ_{ex}/ λ_{em} = 365nm/ 585 nm) or Cu^{2+} (λ_{ex}/ λ_{em} = 365 nm/ 525 nm) as a function of time.

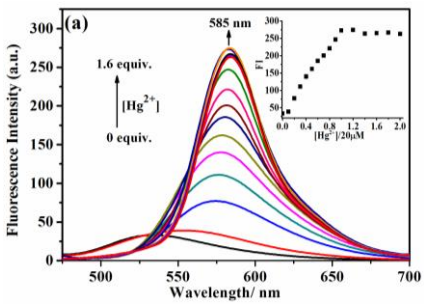

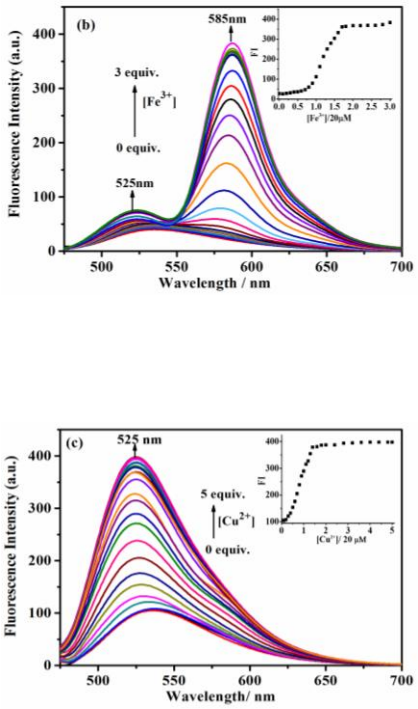

Figure 3. Fluorescence spectral titration of probe **L** (20 μM) with Hg^{2+} (a), Fe^{3+} (b) and Cu^{2+} (c) in CH_3CN/H_2O (97/3, v/v, Tris-HCl, pH 7, measured after stabilization) solution; Inset: the intensity of max wavelength *versus* the added equivalents of Hg^{2+} (a, $\lambda_{ex}/\lambda_{em}$ = 365 nm/ 585 nm), Fe^{3+} (b, $\lambda_{ex}/\lambda_{em}$ = 365 nm/585 nm) and Cu^{2+} (c, $\lambda_{ex}/\lambda_{em}$ = 470 nm/ 525 nm).

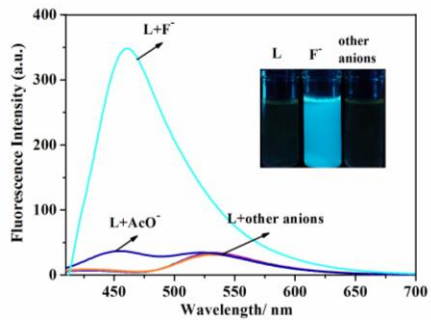

Figure 4. Fluorescence spectrum of probe **L** (20 μM) with 10 equiv. of different anions (F^-, Cl^-, Br^-, I^-, NO^{3-}, HSO_4^-, $H_2PO_4^-$, ClO_4^- and AcO^-) in CH_3CN solution; $\lambda_{ex}/\lambda_{em}$ = 365 nm/ 460 nm.

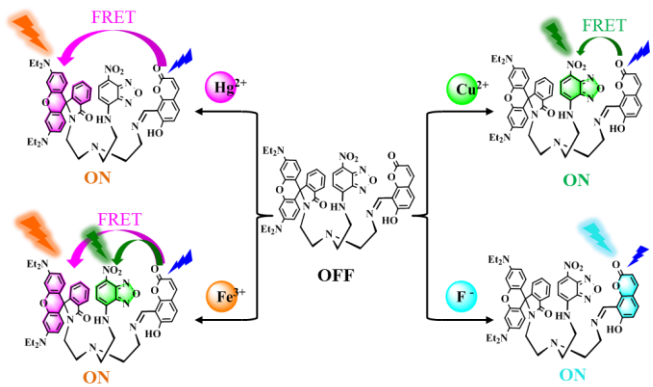

Figure 5. The proposed binding model of the probe **L** with Hg^{2+}, Fe^{3+}, Cu^{2+} and F^- ions.

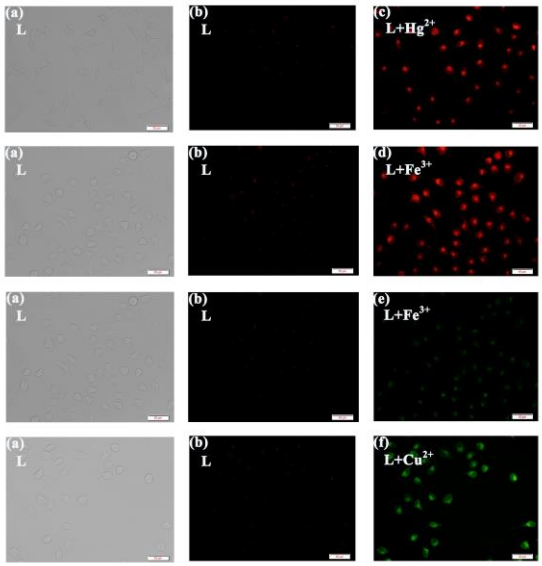

Figure 6. Fluorescence images of ions (50 μM) in live PC3 cells with probe **L** (10 μM). (a) images of cells incubated with probe **L** over 50 min at bright field; (b) fluorescence images of (a) in red or green channel; (c) fluorescence images of cells incubated with probe **L** over 50 min, then with Hg^{2+} over 40 min in red channel; (d) fluorescence images of cells incubated with probe **L** over 50 min, then with Fe^{3+} over 50 min in green channel; (e) fluorescence images of (d) in green channel; (f) fluorescence images of cells incubated with probe **L** over 50 min, then with Cu^{2+} over 50 min in green channel. Red channel: λ_{ex} = 510 nm ~ 550 nm; green channel: λ_{ex} = 450 nm ~ 490 nm.